NASA Technical Memorandum 109097

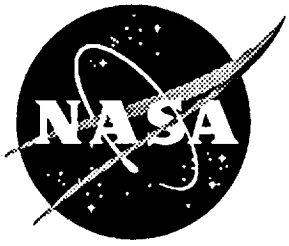

Free Vibration of Thermally Loaded Panels Including Initial Imperfections and Post-Buckling Effects

K. D. Murphy and L. N. Virgin
Duke University, Durham, North Carolina

S. A. Rizzi
NASA Langley Research Center, Hampton, Virginia

April 1994

National Aeronautics and
Space Administration
Langley Research Center
Hampton, Virginia 23681-0001

FREE VIBRATION OF THERMALLY LOADED PANELS INCLUDING INITIAL IMPERFECTIONS AND POST-BUCKLING EFFECTS

Kevin D. Murphy and Lawrence N. Virgin
Department of Mechanical Engineering
Duke University, Durham, NC 27708-0300

Stephen A. Rizzi
NASA Langley Research Center
Structural Acoustics Branch, Hampton, VA 23681-0001

ABSTRACT

A combined theoretical and experimental approach is developed to consider the small amplitude free vibration characteristics of fully clamped panels under the influence of uniform heating. Included in this study are the effects of higher modes, in-plane boundary elasticity, initial imperfections and post-buckling. Comparisons between theory and experiment reveal excellent agreement.

INTRODUCTION

In high performance aerospace applications, the dynamic behavior of plate and shell structures subject to elevated temperatures is a primary concern. Along with damping and loading, the natural frequencies determine the character of the transient response while ordering the steady state response in terms of resonances. In addition, they give insight to the relative stability of these oscillations as described by Croll and Walker [1], i.e. negative eigenvalues imply an unstable response. Clearly, a realistic model for computing the frequencies of these structures at high temperatures is a first step to understanding the entire response of the system.

Early studies in the vibration characteristics of continuous structures concentrated on simply supported buckled beams and high aspect ratio panels under uniaxial compression [2], [3], [4] and [5]. More recently, Gray and Mei [6] used a finite element analysis to consider this problem for flat plates with either simply supported or clamped boundary conditions.

The current paper uses Galerkin's method to develop an analytic model describing the dynamics of fully clamped (out of plane) panels. The in-plane boundary conditions, on the other hand, may be set to allow in-plane displacements at the edges. This is accomplished by restricting the in-plane edge stresses to be proportional to the *average* in-plane edge displacements. Also incorporated into this model are the effects of small initial geometric imperfections. Finally, the behavior of the natural frequencies as a function of temperature, spanning the pre and post-buckled regime, is considered. An experimental study was also conducted to measure the natural frequencies. These results are presented and compared to the theoretical findings.

THEORETICAL APPROACH

Equation of Motion and Solution Technique

The von Karman nonlinear partial differential equation governing the panel's behavior is used in this study. It may be written in nondimensional form [7]

$$\acute{\nabla}^4 w - \left(\frac{a_x}{b_y}\right)^2 \left[\frac{\partial^2 F}{\partial \eta^2}\left(\frac{\partial^2 w}{\partial \xi^2} + \frac{\partial^2 w_0}{\partial \xi^2}\right) + \frac{\partial^2 F}{\partial \xi^2}\left(\frac{\partial^2 w}{\partial \eta^2} + \frac{\partial^2 w_0}{\partial \eta^2}\right) - 2\frac{\partial^2 F}{\partial \xi \partial \eta}\left(\frac{\partial^2 w}{\partial \xi \partial \eta} + \frac{\partial^2 w_0}{\partial \xi \partial \eta}\right)\right] + \frac{\partial^2 w}{\partial \tau^2} + C\frac{\partial w}{\partial \tau} + \Delta P = 0 \tag{1}$$

where w is the lateral displacement of the panel, w_0 is the initial imperfection, F is the Airy stress function, C is the system damping and ΔP is the external loading. In addition, ξ and η are the nondimensional coordinates

$$\xi = \frac{x}{a_x} \qquad \eta = \frac{y}{b_y}$$

and a_x and b_y are the length and width of the panel, respectively. The associated compatibility equation relating the in-plane stress resultants to the lateral displacements takes the form

$$\acute{\nabla}^4 F = 12(1-\nu^2)\left(\frac{a_x}{b_y}\right)^2 \left[\left(\frac{\partial^2 w}{\partial \xi \partial \eta}\right)^2 + 2\left(\frac{\partial^2 w}{\partial \xi \partial \eta}\right)\left(\frac{\partial^2 w_0}{\partial \xi \partial \eta}\right) - \frac{\partial^2 w}{\partial \xi^2}\frac{\partial^2 w}{\partial \eta^2} - \frac{\partial^2 w}{\partial \xi^2}\frac{\partial^2 w_0}{\partial \eta^2} - \frac{\partial^2 w}{\partial \eta^2}\frac{\partial^2 w_0}{\partial \xi^2}\right] \tag{2}$$

where ν is Poisson's ratio. For a complete discussion of these equations see Dowell [7].

In an attempt to obtain a solution for the displacement field, a two step solution procedure is taken which expands on the method developed by Ventres and Dowell [8]. For this procedure, a one mode initial imperfection and a nine-mode expansion for the displacement field are assumed to take the form

$$w_0(\xi,\eta) = \tilde{a}_{mn}\tilde{\Psi}_m(\xi)\tilde{\Phi}_n(\eta)$$

$$w(\xi,\eta,\tau) = \sum_{i=1}^{3}\sum_{j=1}^{3} a_{ij}(\tau)\Psi_i(\xi)\Phi_j(\eta) \tag{3}$$

where $\Psi_i(\xi)$ and $\Phi_j(\eta)$ are spatial beam mode shapes which satisfy the zero deflection, zero slope boundary conditions for a fully clamped panel. Throughout the course of this study the modes were assumed to be

$$\Psi_i(\xi) = \cos([i-1]\pi\xi) - \cos([i+1]\pi\xi)$$

$$\Phi_j(\eta) = \cos([j-1]\pi\eta) - \cos([j+1]\pi\eta) \tag{4}$$

The first step is to obtain a solution to the compatibility equation. The *particular* solution is found by substituting the assumed displacement field (Equation (3)) into

Equation (2) and writing F_p as an expansion in terms of the spatial modes, $\Phi_i(\xi)$ and $\Psi_j(\eta)$. As a result, the particular solution does not contribute to the in-plane load at the boundaries (since the mode shapes are zero there). The *homogeneous* solution, F_h, must account for the contribution at the edges. This is accomplished by enforcing an "average" force-displacement boundary condition. This takes the form

$$\frac{\partial^2 F_h}{\partial \eta^2} = -\left(\frac{a_x}{h_z}\right) K_\xi \int_0^1 \Delta_\xi d\eta$$

$$\frac{\partial^2 F_h}{\partial \xi^2} = -\left(\frac{b_y}{h_z}\right) K_\eta \int_0^1 \Delta_\eta d\xi \tag{5}$$

where the Δ's are the in-plane edge displacements, h_z is the panel thickness and the K's are in-plane edge stiffnesses (distributed in-plane springs). This formulation, therefore, allows for finite in-plane displacements at the boundaries. A detailed description of the procedure for determining the Airy stress function, F, is provided in [9].

The second step in the solution procedure is to carry out Galerkin's method on the panel equation of motion. This involves substituting the expressions for w and w_0, Equation (3), and the Airy stress function, F, into the partial differential equation of motion, Equation (1). The resulting expression is then multiplied by the modal functions, $\Psi_r(\xi)$ and $\Phi_s(\eta)$, and integrated over the domain. This integration removes all spatial dependence and leaves the following set of equations

$$[M]\ddot{\vec{x}} + C[M]\dot{\vec{x}} + f(\vec{x}) = \vec{P} \tag{6}$$

where $[M]$ is a coupled mass matrix, C is a scalar damping term (assuming proportional damping), f is a nonlinear stiffness term, $\vec{P}$ is an excitation vector and $\vec{x}$ is a vector containing the nine modal coefficients, a_{ij}. This is a set of nine coupled nonlinear ordinary differential equations governing the modal coefficients.

Natural Frequencies

First, consider the natural frequencies at the ambient temperature. After omitting the damping and excitation terms in Equation (6), the resulting set of equations are linearized by expanding the nonlinear stiffness in a Taylor series about the static equilibrium vector, $\vec{x}_{eq} = \vec{0}$, and discarding higher order terms [10]. The resulting system of equations take the form

$$[M]\ddot{\vec{x}} = -[J]\vec{x} \tag{7}$$

where $[J]$ is the Jacobian representing the linearized stiffness. The elements of $[J]$ are given by

$$J_{ij} = \left.\frac{\partial f_i}{\partial x_j}\right|_{\vec{x}_{eq}} \tag{8}$$

From Equations (7) and (8), the standard dynamic eigenvalue problem results [11]. The nine eigenvalues, associated with the equilibrium configuration, are then computed numerically.

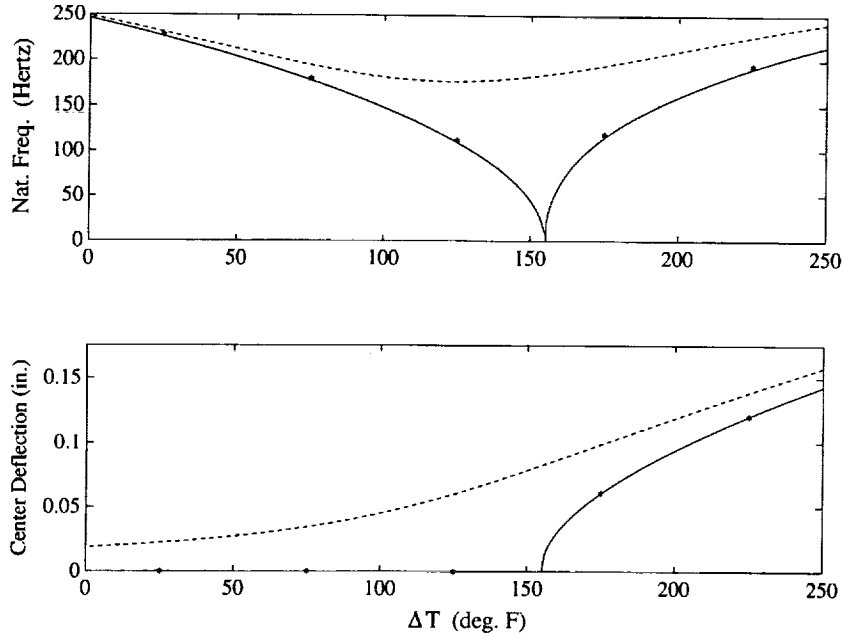

Figure 1: Typical flat plate (—) and initially imperfect plate (- -) responses to thermal loads and comparison with Finite Element Results (*).

The temperature is then incremented and the new equilibrium vector is found by setting the entire nonlinear stiffness to zero. This set of nonlinear coupled algebraic equations is then solved with a Newton-Raphson algorithm using the equilibrium configuration at the previous temperature as an initial guess vector. Next, the stiffness is linearized about the new equilibrium state and a new set of eigenvalues are computed for this temperature and so on.

The one deviation in this scheme occurs for an initially flat panel (i.e. no initial imperfection). Here, the above procedure is carried out until one eigenvalue becomes negative. This indicates a loss of stability of the flat plate equilibrium configuration [1]. As a result, the new stable equilibrium position must be found using the Newton-Raphson scheme. This is accomplished by perturbing the initial guess vector in the direction of the unstable eigenvector (the eigenvector associated with the negative eigenvalue). This allows the Newton-Raphson routine to find the non-zero equilibrium configuration about which the system will be linearized in order to obtain the post-buckled natural frequencies.

The panel under consideration had dimensions of 15in x 12in x 0.125in (aspect ratio = 1.25) and was made of AISI 321 stainless steel. The material properties of this steel include $E = 28\text{x}10^6\text{psi}$, $\nu = 0.33$, $\alpha = 9.6\text{x}10^{-6}$ (in/in)/°F and $\rho = 0.29\text{lb/in}^3$. A typical frequency result displaying the behavior of the fundamental mode is shown in Figure 1a. For the perfectly flat panel, the frequencies decrease until instability is encountered at a change in temperature of $\Delta T_{cr} \approx 155.25$ °F after which the frequencies begin to rise again. The loss of stability of the flat plate equilibrium position at this critical temperature is clearly displayed by Figure 1b which shows the center deflection as

a function of temperature. Also shown are the "stiffening" effects of initial imperfections. This case shows a panel with an initial center deflection of 0.038in (see $\Delta T = 0$). Because the system has a finite displacement even below ΔT_{cr} (as displayed in Figure 1b), there is never a distinct bifurcation, as in the flat plate configuration, and the eigenvalues never become negative [12]. This is properly displayed by Figure 1a.

In addition, a finite element package was used to independently verify these results at discrete temperatures for the initially flat panel. See Figure 1a and 1b.

EXPERIMENTAL APPROACH

Facilities

The experimental portion of this work was conducted in the Thermal Acoustic Fatigue Apparatus (TAFA) [13] at NASA Langley. TAFA is a progressive wave tube facility for testing small panels subject to thermal and/or acoustic excitations.

The acoustic excitation in TAFA is provided by a set of air modulators coupled by an exponential horn to a 6ft x 6ft x 1ft test section. Within the test section, specimens are mounted on a side wall and, thus, are subject to a grazing acoustic load. The system is capable of providing both sinusoidal and broadband excitation in the range of 40-500Hz. Overall sound pressure levels between 125dB and 165dB can be generated in the TAFA facility.

Directly across the chamber from the test specimen is an 18in x 28in x 1in thick quartz window behind which are a set of ten quartz lamp units used to provide thermal loads to the panel. Using all 10 lamps, this configuration is capable of generating a maximum heat flux of 45 BTU/(ft^2 sec). Thin panels can be heated to over 2000 $^\circ F$. In addition, a low velocity mean flow is employed to minimize natural convection and produce a more spatially uniform temperature distribution [13].

The mounting frame, attached to the side wall of the test section, was designed specifically for this experiment and very nearly provided the zero deflection, zero slope boundary conditions of an ideally clamped panel. The frame design was complicated by the fact that both frame and panel were made of the same material. This would result in an unavoidable and undesirable expansion of the frame along with the panel during heating. Several steps were taken to minimize this effect. Insulating blanket material (Min-K) was placed on the inside wall of the test section surrounding the panel to minimize thermal conduction through the wall to the support frame. Zircar, a ceramic insulation material, was placed between the test panel and the frame to help minimize conduction between the panel and the frame. Finally, a water channel was mounted on the inside of the frame to provide continuous cooling in the vicinity of the largest thermal radiation from the panel. During the course of the experiments, the temperature of the water cooled facility was monitored using thermocouples and, although the frame did heat up, the safeguards taken seemed to prevent appreciable heating. For instance, in one series of tests, the panel was heated to 315 $^\circ F$ above ambient while the temperature of the water cooled system only went up about 10 $^\circ F$.

The test panel was instrumented with several thermocouples to ascertain the temperature distribution and strain gages were used to determine the dynamic response.

Temperature data from the panel and mounting frame were recorded continuously on a computer. By adjusting the lamp bank energy distribution, a nearly uniform temperature field was obtained on the panel.

Dynamic strain measurements were recorded on a multi-channel spectrum analyzer. Frequency response functions were generated between the strains and the acoustic load, as measured by a pair of microphones, to determine the resonant frequencies. In addition to the strain gages, a scanning laser vibrometer was used to determine the out-of-plane RMS velocity distribution over the panel [14]. The laser vibrometer gives a measure of the instantaneous velocity response at a point by measuring the doppler shift between the reference beam and reflected beam. Spatial information may be determined by directing the laser spot across many points over the panel using a set of positioning mirrors. A PC based acquisition system [14] was used to move the beam sequentially over a series of "grid points" on the panel. The RMS velocity is computed at each point and stored on the PC. By exciting the structure at one of its resonances, a rectified distribution resembling the mode shape was obtained.

Experimental Procedure

Beginning at the ambient temperature, a low level, broadband acoustic input was used to excite the panel. The frequency response functions were generated and used to identify resonant frequencies. Based on this information alone, it is impossible to associate a given frequency with it's mode shape. This problem is complicated by the fact that non-panel frequencies will also be present in the response. Indeed, the test section wall has resonances which appear in the frequency response. To resolve this difficulty each frequency peak was considered individually. Using a narrow band acoustic excitation at the i^{th} resonant frequency, the panel was forced to oscillate primarily in the i^{th} mode. A laser vibrometer scan was then made to show the rms velocity field. From this velocity field, the mode shape related to that frequency was evident (since velocity and displacement are out of phase by 90°). Two typical scans are shown in Figure 2a and 2b where the (2,1) and the (3,2) modes, respectively, are clearly visible.

Once all the peaks had been identified, the temperature was increased and the above procedure was carried out again. By identifying each frequency and its corresponding mode shape, the response as a function of temperature, can be inferred with a high degree of confidence.

RESULTS

The following results were obtained using a panel with the same dimensions and material properties as described previously. At the time of the experiment, the ambient temperature was 67.5 $°F$.

Figure 3a presents the experimental frequency results as a function of temperature. It is evident that none of the experimental frequencies come particularly close to zero. This is not due to the less than perfectly clamped out of plane boundary conditions. While this effect would tend to decrease the frequencies at a given temperature, it would not change the character of the results. Therefore, the fact that the experimental

a)

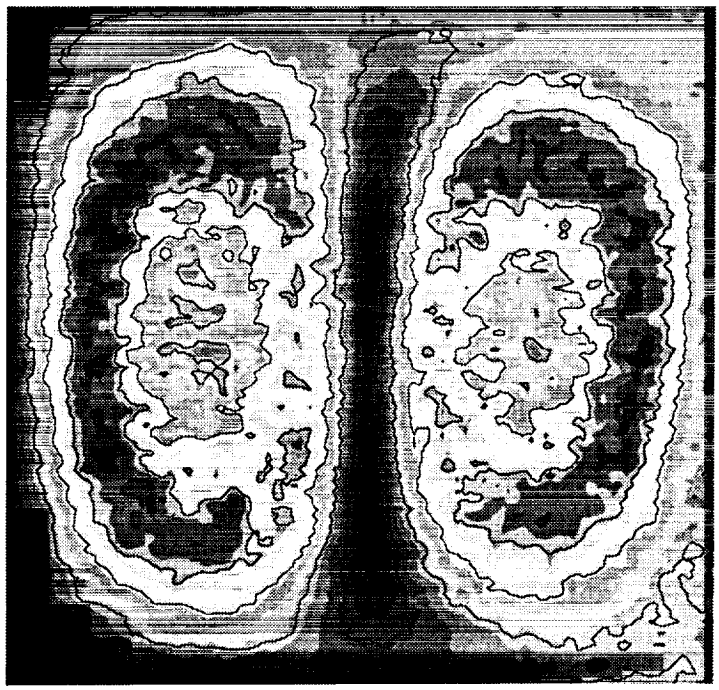

b)

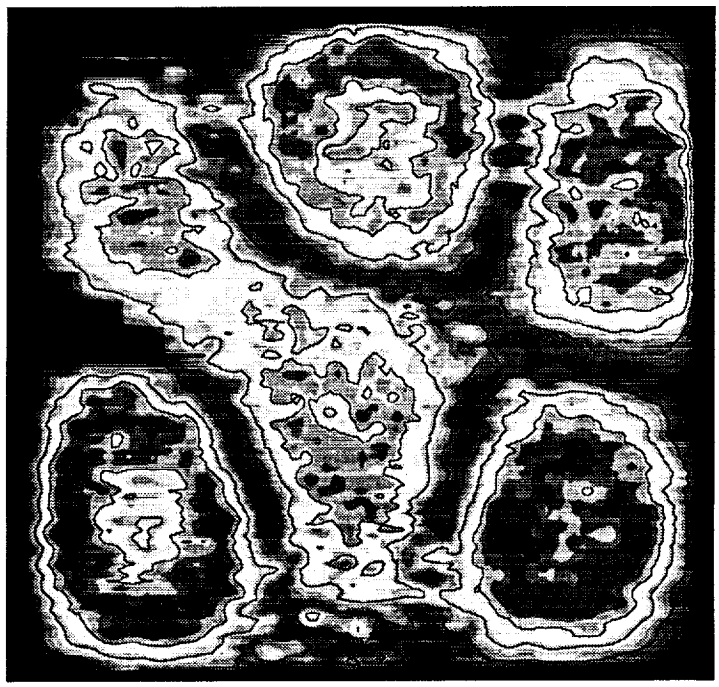

Figure 2: The rms velocity field as measured using the Vibration Pattern Imager. a) the (2,1) mode and b) the (3,2) mode.

a)

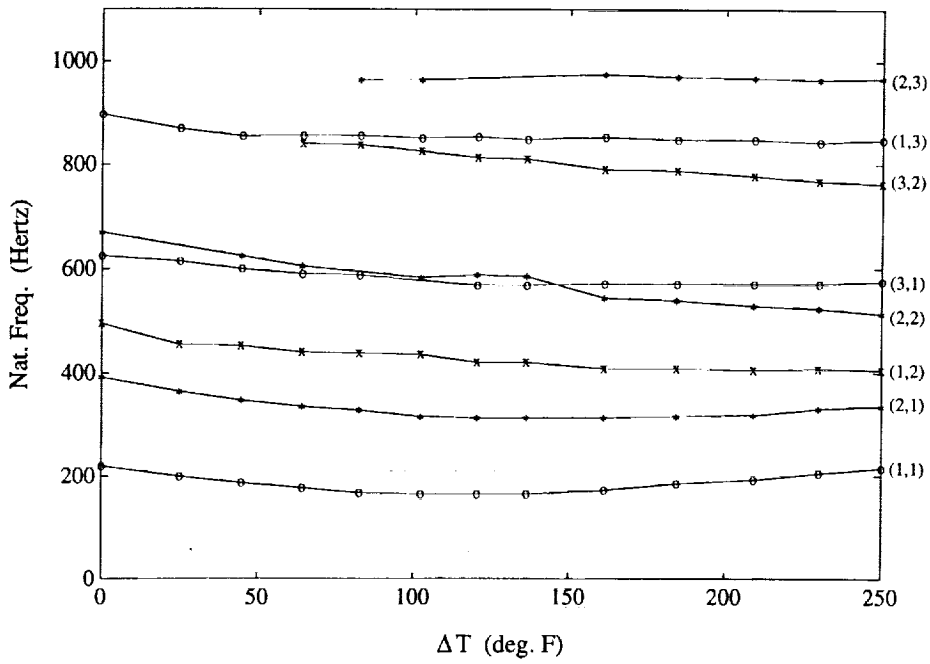

b)

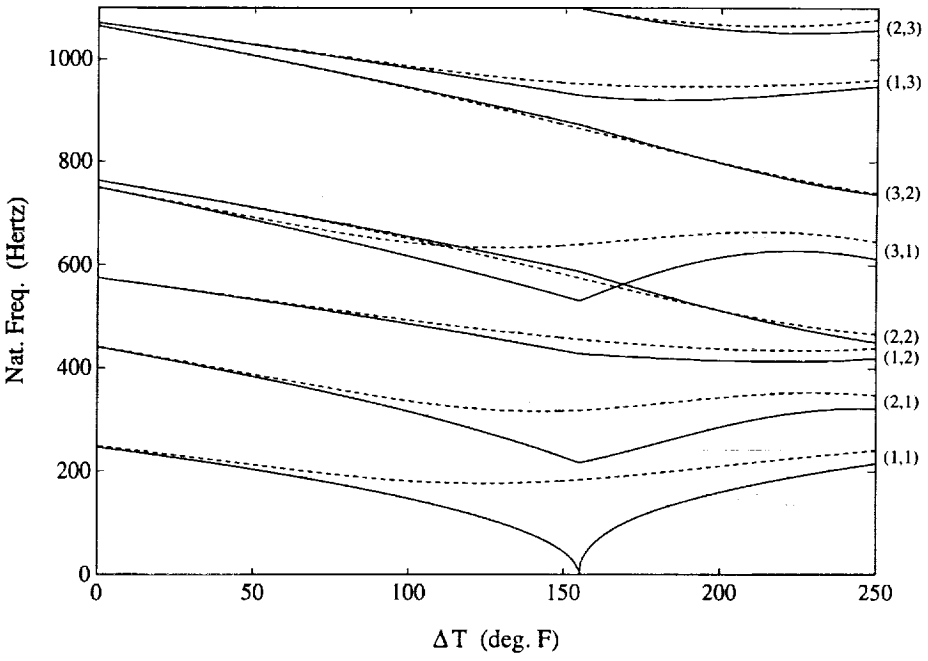

Figure 3: Natural frequencies of the panel as a function of temperature. Designations on the right give an indication of the dominant mode. a) experimental results. b) theoretical results: initially flat (—) and imperfect (- -).

frequencies do not drop to zero implies the presence of an initial imperfection, which would be expected in the present system.

Figure 3b shows the theoretical frequency-temperature results for the flat plate and the initially imperfect panel. These results were determined using a finite in-plane edge stiffness, whose value was based on matching the theoretical critical buckling temperature with experimental observations. Experimentally, the finite edge stiffness is, most likely, due to the inability of the ceramic insulation material to prevent in-plane displacements. Based on this figure, the flat panel buckles in the (1,1) mode at a critical temperature of $\Delta T_{cr} \approx 155.25\ ^{\circ}F$. The results for the imperfect panel are based on the assumption that the imperfection is in the shape of the (1,1) mode (see Equation (3)) with an amplitude $\tilde{a}_{11} = 0.038$. This corresponds to an initial deflection of 0.019in at the center of the plate (15% of the thickness).

A comparison of the experimental and theoretical results is revealing. Quantitatively, the (1,1) frequencies are in good agreement. This agreement becomes increasingly less impressive for the higher frequencies. This is entirely expected in a study with a limited number of modes. Including additional modes would improve the agreement between the theoretical and experimental results for the higher modes shown in Figure 3. Quantitative comparisons from these results should be limited to the first three or four modes.

The qualitative similarities between theory and experiment for all the modes is evident. Both Figure 3a and 3b show a significant gap between the (2,1) and (1,2) frequency loci. Furthermore, the crossing of the (3,1) and (2,2) loci occurs experimentally near a temperature increase of $142.5\ ^{\circ}F$ and is predicted by theory albeit at a lower temperature ($\Delta T = 115\ ^{\circ}F$). Clearly, the theoretical model contains the essential dynamics which are responsible for the behavior of the frequencies as a function of temperature.

Based on these figures, it might appear that there are no appreciable variations in the natural frequencies with temperature. However, there are, and to highlight this fact Figure 4 compares the experimental and theoretical results for the (1,1) mode on a more reasonable frequency scale. There is about a 20% variation in the fundamental frequency with temperature.

DISCUSSION

This paper presented a combined theoretical and experimental study into the behavior of the natural frequencies of a panel subject to thermal loads.

Comparisons between theory and experiment show reasonable quantitative agreement between the lower eigenvalues. The higher eigenvalues, on the other hand, differ more noticably. This is partly attributed to the relatively few modes used in the course of the theoretical analysis. However, there is excellent qualitative agreement, even in the higher modes, implying that the model captured the relevant dynamics of the problem.

The differences between the experimental and numerical results are partly a reflection of our inability to accurately model the boundary conditions of the experimental setup. Considerable effort was spent determining the in-plane boundary stiffness and the initial imperfection. Because K_ξ and K_η were based on static information over a range

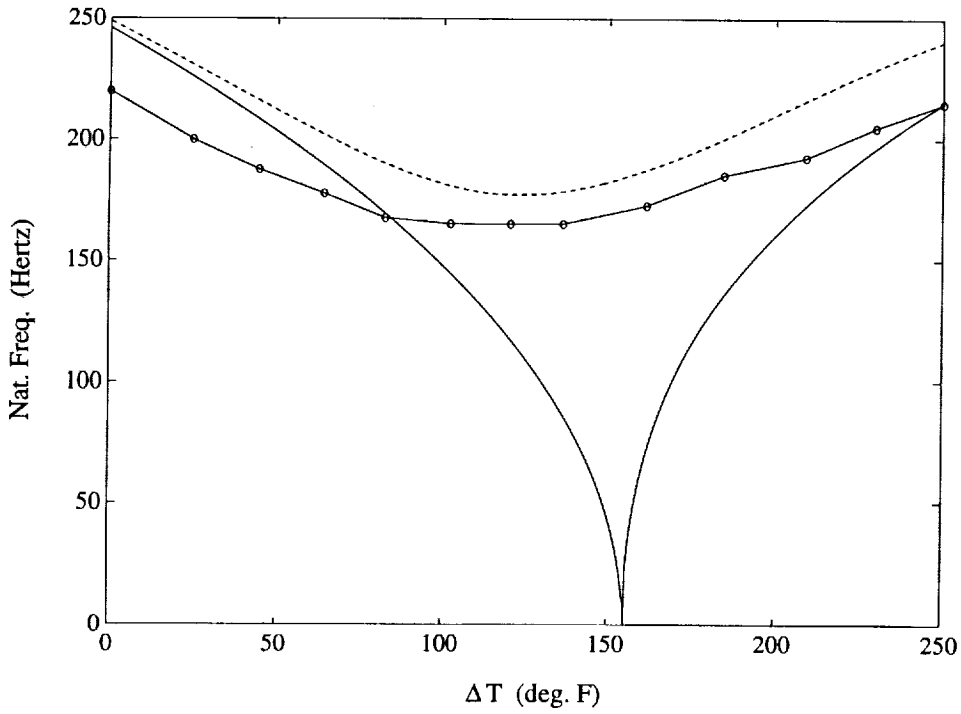

Figure 4: Comparison of the theoretical and experimental frequencies (o) for the fundamental mode.

of temperatures, the frequency-temperature results are not expected to match exactly at any given ΔT. Furthermore, because the analysis uses an "average" force-displacement condition on the edges, local boundary effects, which may significantly influence the panels dynamic behavior, are not considered. Also contributing to these differences are such factors as prestress in the panel (induced during clamping), nonuniform temperature distributions and variations in temperature through the panels thickness. This formulation does have several advantages over, say, a finite element analysis. Because this study develops the equations of motion for the panel (Equation (1)) using analytic expressions, additional insight may be gained into the effects of such terms as the temperature rise, ΔT, the in-plane boundary stiffnesses, K_ξ, K_η, the initial imperfection (both shape and magnitude) and so on. Also, the Galerkin technique is an efficient (computationally fast) method for computing the natural frequencies particularly for small temperature increments (see Figure 1a and 1b). Finally, this formulation may easily be extended to consider other aspects of the dynamic problem, most notably the forced case. In addition, the results of this study provide important information about a portion of the parameter space, (T, ω), for the forced problem.

REFERENCES

[1] J.G.A. Croll and A.C. Walker, 1972. *Elements of Structural Stability*, Wiley and Sons, New York.

[2] R.L. Bisplinhoff and J. Dugundji, 1958. *High Temperature Effects in Aircraft Structures*, Chapter 14, 288-312, Influence of Aerodynamic Heating on Aeroelastic Phenomena, Pergamon Press.

[3] R.L.Bisplinghoff and T.H.H. Pian, 1956. *9th International Congress of Applied Mechanics*, **7**, 307-318. On the Vibrations of Thermally Buckled Bars and Plates.

[4] H. Lurie, 1952. *Journal of Applied Mechanics*, 195-204. Lateral Vibration as Related to Structural Stability.

[5] C.F. Ng and R.G. White, 1988. *Journal of Sound and Vibration*, **120**, 1, 1-18. Dynamic Behaviour of Postbuckled Isotropic Plates Under In-Plane Compression.

[6] C.C. Gray and C. Mei, 1991. *32nd Structures, Structural Dynamics and Materials Conference* Finite Element Analysis of Thermal Post-Buckling and Vibrations of Thermally Buckled Composite Plates.

[7] E.H. Dowell, 1975. *Aeroelasticity of Plates and Shells*, Noordhoff International Publishing (now Kluwer).

[8] C.S. Ventres and E.H. Dowell, 1970. *AIAA Journal*, **8**, 11, 2022-2030. Comparison of Theory and Experiment for Nonlinear Flutter of Loaded Plates.

[9] K.D. Murphy, L.N. Virgin and S.A. Rizzi, 1994. To be published in *AIAA Journal*, A Theoretical Investigation of the Free Vibration Characteristics of Thermally Loaded Square Panels.

[10] S. Wiggins, 1989. *Introduction to Applied Nonlinear Dynamical Systems and Chaos*, Springer-Verlag.

[11] L.E. Meirovitch, 1984. *Analytic Methods in Vibrations*, Wiley and Sons, London.

[12] L.N. Virgin, 1985. *International Journal of Mechanical Science*, **27**, 4, 235-248. The Dynamics of Symmetric Post-Buckling.

[13] S.A. Clevenson and E.F. Daniels, 1992. *NASA Technical Memorandum 104106*, Capabilities of the Thermal Acoustic Fatigue Apparatus.

[14] S.A. Rizzi, D.E. Brown and T.A. Shaffer, 1993. *NASA Technical Memorandum 107721*, VPI: Vibration Pattern Imager.

REPORT DOCUMENTATION PAGE

Form Approved
OMB No. 0704-0188

1. AGENCY USE ONLY (*Leave blank*)	2. REPORT DATE	3. REPORT TYPE AND DATES COVERED
	April 1994	Technical Memorandum

4. TITLE AND SUBTITLE
Free Vibration of Thermally Loaded Panels Including Initial Imperfections and Post-Buckling Effects

5. FUNDING NUMBERS
WU 505-63-50-10

6. AUTHOR(S)
K. D. Murphy
L. N. Virgin
S. A. Rizzi

7. PERFORMING ORGANIZATION NAME(S) AND ADDRESS(ES)
NASA Langley Research Center
Hampton, VA 23681-0001

8. PERFORMING ORGANIZATION REPORT NUMBER

9. SPONSORING / MONITORING AGENCY NAME(S) AND ADDRESS(ES)
National Aeronautics and Space Administration
Washington, DC 20546

10. SPONSORING / MONITORING AGENCY REPORT NUMBER
NASA TM-109097

11. SUPPLEMENTARY NOTES
Murphy and Virgin: Duke University, Durham, NC
Rizzi: NASA Langley Research Center, Hampton, VA
Note: Paper submitted for presentation at the Fifth International Conference on Recent Advances in Structural Dynamics, Southampton, England, 7/18-21/94.

12a. DISTRIBUTION / AVAILABILITY STATEMENT
Unclassified — Unlimited
Subject Category — 71

12b. DISTRIBUTION CODE

13. ABSTRACT (*Maximum 200 words*)

A combined theoretical and experimental approach is developed to consider the small amplitude free vibration characteristics of fully clamped panels under the influence of uniform heating. Included in this study are the effects of higher modes, in-plane boundary elasticity, initial imperfections and post-buckling. Comparisons between theory and experiment reveal excellent agreement.

14. SUBJECT TERMS
Thermal Buckling; Initial Imperfection; Free Vibration; Natural Frequencies

15. NUMBER OF PAGES
12

16. PRICE CODE
A03

17. SECURITY CLASSIFICATION OF REPORT	18. SECURITY CLASSIFICATION OF THIS PAGE	19. SECURITY CLASSIFICATION OF ABSTRACT	20. LIMITATION OF ABSTRACT
Unclassified	Unclassified	Unclassified	